UROGENITAL

Influence of imaging and histological factors on prostate cancer detection and localisation on multiparametric MRI: a prospective study

**Flavie Bratan · Emilie Niaf · Christelle Melodelima ·
Anne Laure Chesnais · Rémi Souchon ·
Florence Mège-Lechevallier · Marc Colombel ·
Olivier Rouvière**

Abstract

Objectives To assess factors influencing prostate cancer detection on multiparametric (T2-weighted, diffusion-weighted, and dynamic contrast-enhanced) MRI.

F. Bratan · O. Rouvière
Department of Urinary and Vascular Radiology, Hôpital Edouard
Herriot, Hospices Civils de Lyon, Lyon 69437, France

F. Bratan · E. Niaf · R. Souchon · O. Rouvière
LabTau, Inserm, U1032, Lyon 69003, France

C. Melodelima
Laboratoire d'Ecologie Alpine, CNRS UMR 5553, Université
Joseph Fourier, BP 53, Grenoble 38041, France

A. L. Chesnais · F. Mège-Lechevallier
Department of Pathology, Hôpital Edouard Herriot, Hospices
Civils de Lyon, Lyon 69437, France

M. Colombel · O. Rouvière
Université de Lyon, Lyon 69003, France

M. Colombel · O. Rouvière
Faculté de Médecine Lyon Est, Université Lyon 1,
Lyon 69003, France

M. Colombel
Department of Urology, Hôpital Edouard Herriot,
Hospices Civils de Lyon, Lyon 69437, France

O. Rouvière (✉)
Service de Radiologie Urinaire et Vasculaire, Pavillon P,
Hôpital E. Herriot, 5 Place d'Arsonval 69437,
Lyon Cedex 03, France
e-mail: olivier.rouviere@netcourrier.com

E. Niaf
CREATIS, CNRS UMR5220, Inserm U1044, INSA-Lyon,
Villeurbanne 69100, France

Methods One hundred and seventy-five patients who underwent radical prostatectomy were included. Preoperative MRI performed at 1.5 T ($n=71$) or 3 T ($n=104$), with ($n=58$) or without ($n=117$) an endorectal coil were independently interpreted by two radiologists. A five-point subjective suspicion score (SSS) was assigned to all focal abnormalities (FAs). MR findings were then compared with whole-mount sections.
Results Readers identified 192–214/362 cancers, with 130–155 false positives. Detection rates for tumours of <0.5 cc (cm^3), 0.5–2 cc and >2 cc were 33–45/155 (21–29 %), 15–19/35 (43–54 %) and 8–9/12 (67–75 %) for Gleason ≤6, 17/27 (63 %), 42–45/51 (82–88 %) and 34/35 (97 %) for Gleason 7 and 4/5 (80 %), 13/14 (93 %) and 28/28 (100 %) for Gleason ≥8 cancers respectively. At multivariate analysis, detection rates were influenced by tumour Gleason score, histological volume, histological architecture and location ($P<0.0001$), but neither by field strength nor coils used for imaging. The SSS was a significant predictor of both malignancy of FAs ($P<0.005$) and aggressiveness of tumours ($P<0.00001$).
Conclusions Detection rates were significantly influenced by tumour characteristics, but neither by field strength nor coils used for imaging. The SSS significantly stratified the risk of malignancy of FAs and aggressiveness of detected tumours.
Key Points
• *Prostate cancer volume, Gleason score, architecture and location are MRI predictors of detection.*
• *Field strength and coils used do not influence the tumour detection rate.*
• *Multiparametric MRI is accurate for detecting aggressive tumours.*
• *A subjective suspicion score can stratify the risk of malignancy and tumour aggressiveness.*

🖄 Springer

Abbreviations

Mp-MRI	Multiparametric magnetic resonance imaging
T2w imaging	T2-weighted imaging
Dw imaging	Diffusion-weighted imaging
DCE imaging	Dynamic contrast enhanced imaging
MRS	Magnetic resonance spectroscopy
FA	Focal abnormality
FP	False positive
FN	False negative
TP	True positive
SSS	Subjective suspicion score
PZ	Peripheral zone
TZ	Transition zone
ADC	Apparent diffusion coefficient
OR	Odds ratio
PSA	Prostate-specific antigen
PPA	Pelvic phased-array

Introduction

Detecting and localising cancer foci within the prostate is critical. Indeed, the precise mapping of prostate cancer could increase biopsy sensitivity, allow a more rational selection and follow-up of patients under active surveillance, improve treatment planning and allow the development of focal therapies aimed at destroying tumour foci while preserving the rest of the gland [1, 2].

Multiparametric magnetic resonance imaging (mp-MRI) combining T2-weighted (T2w) imaging with diffusion-weighted (Dw) imaging, dynamic contrast-enhanced (DCE) imaging and/or magnetic resonance spectroscopy (MRS) has yielded promising results in prostate cancer detection and localisation [3–6].

However, there still is a lack of consensus with regard to the use of prostate mp-MRI and some urologists think it is not ready for routine use yet [7]. As a result, many groups have tried to evaluate the factors that influence mp-MRI performances and particularly the characteristics of tumours that can be missed on mp-MRI as well as the causes of false positive (FP) findings. There is an increasing body of evidence suggesting that prostate cancer location and histological characteristics (such as Gleason score, volume and architecture) influence its ability to be detected on mp-MRI [8–16]. Conversely, the impact of imaging factors, and particularly of the field strength and the coils used, on mp-MRI cancer detection has been less studied and remains a matter of debate [17–21].

Similarly, potential causes of FP findings have been specifically evaluated only in a few studies [9, 22].

In 2008, we started a prospective database collecting mp-MRI and histopathological findings in patients treated by radical prostatectomy. Its primary purpose was to assess, using precise MR pathological correlations, the mp-MRI prostate cancer detection rates as a function of tumour Gleason score, volume, location and histological architecture. The secondary objective was to define the histological conditions explaining FP findings on mp-MRI. We report here the results obtained in 175 patients.

Materials and methods

Study population

At our institution, prostate MRI is part of the usual preoperative work-up before prostatectomy. Since September 2008, all patients treated by prostatectomy who had undergone a preoperative prostate MRI at our institution were proposed to have their data entered in a radio-pathological correlation database (CLARA-P database). Formal approval by our Institutional Review Board (IRB) was not required for this observational study. Nevertheless, the IRB reviewed the informed form and all included patients gave written informed consent. The database was also registered with the appropriate administrative authority (Commission Nationale de l'Informatique et des Libertés, no. 08-06), as requested by our national law. In total, 175 consecutive patients were included. Their mean age and prostate-specific antigen (PSA) level were 61.3 years (45–73 years) and 8.75 ng/ml (0.9–60 ng/ml).

MR protocol

All mp-MRI included T2w, Dw and DCE imaging. Patients were imaged in two departments of radiology at our institution. Department 1 had 1.5-T MRI until March 2010 (device A, $n=71$) and 3-T MRI (device B, $n=46$) thereafter, and used a pelvic phased array (PPA) coil only for prostate imaging; Department 2 used a 3-T MRI (device C, $n=58$) and combined endorectal and PPA coils throughout the study. There was no particular patient selection about the MRI allocation.

MR image acquisition parameters are detailed in Table 1. T2w images were obtained in the axial and sagittal planes and Dw and DCE images in the axial plane only. For Dw imaging, maximum b values ranged from 600 to 2,000 s/mm^2. These b values were mainly chosen to keep an acceptable signal-to-noise ratio on apparent diffusion coefficient (ADC) maps, depending on the field strength and coil configuration. For DCE imaging, an intravenous injection of 0.2 ml/kg of gadoterate meglumine (Dotarem; Guerbet, Roissy, France) was performed at 3 ml/s in all cases. Temporal resolution was adapted to the field strength and coil configuration.

Table 1 MRI parameters at 1.5 T and 3 T

Scanner	A			B			C		
Manufacturer, field strength	Siemens Medical Systems, 1.5 T			General Electric Medical Systems, 3 T			Philips Medical Systems, 3 T		
Model name	Symphony 2004A			Discovery MR750			Achieva 3 T Xseries		
Receive coil type	16-channel PPA coil			32-channel PPA coil			16-channel PPA+endorectal coil		
Sequence	T2w	Dw	DCE	T2w	Dw	DCE	T2w	Dw	DCE
Repetition time (ms)	7750	4800	5.38	5,000	5,000	3.9	5,021	3,925	4
Echo time (ms)	109	90	2.73	104	90	1.7	120	70	2.3
Field of view (mm^2)	200×200	300×300	240×240	220×220	380×380	240×192	180×180	180×180	180×180
Acquisition matrix	256×184	128×83	256×135	384×256	128×128	180×160	344×255	116×103	100×100
Flip angle (degrees)	90/180	90	10	90/180	90	12	90/180	90	8
b values (s/mm^2)		0, 600			0, 2,000			0, 800, 2,000	
Section thickness (mm)	3	3	3	3	3	3	3	3	3
Number of temporal acq.		12			32			50	
Temporal resolution (s)		15			7			5	

PPA Pelvic phased-array, *T2w* T2-weighted imaging, *Dw* diffusion-weighted imaging, *DCE* dynamic contrast-enhanced imaging, *acq* acquisitions

T2w, Dw and DCE axial images were acquired with the same slice thickness and position in order to allow direct comparison between sequences.

Preparation of the prostatectomy specimens

After 24 h in formaldehyde solution and conisation of the apex and bladder neck for margins analysis, the prostate was strictly cut from apex to base in an axial plane using a specifically designed machine that ensured that the blocks were evenly spaced. The blocks obtained were put in formaldehyde for a further 24- to 48-h fixation period, processed and paraffin embedded as whole-mounts.

Whole-mount sections were usually obtained every 1–1.5 mm and their precise location within the blocks was monitored. Then, they were stained with haematoxylin-eosin.

Histopathological analysis

One uropathologist with 10 years of experience at the start of the database in 2008 reviewed the whole-mount sections. She was blinded to all MR data.

Tumours were localised using the same dedicated diagram as radiologists. Gleason score was assessed for all tumour foci. Tumour architecture was classified into four categories: dense cancers (continuous malignant tissue with minimal intervening benign glands), infiltrative cancers (rare and spaced tumoral glands intermixed with benign glands with no dense tumoral component), mixed cancers (dense and infiltrative tumoral components) and lobulated cancers (well-differentiated transition zone cancers).

Only individual tumours with minimum in-plane dimensions of $2×2 mm^2$, visible on at least two section levels and with a Gleason score ≥5 were delineated on each section; others were not taken into consideration. Malignant regions that were less than 1 mm apart from each other in the same plane, with the same architecture and Gleason score were considered to be parts of the same tumour. Tumour limits (including infiltrative components) were outlined on the whole-mount sections by the pathologist. Then, 3-mm spaced whole-mount sections were selected for MR-pathological correlation and digitised alongside a ruler for calibration purpose. The volume of all tumours was calculated on digitised sections using dedicated in-house software (Matlab; Mathworks, Natick, MA USA).

MR image analysis

MR images of the patients included in the database were all independently reviewed by the same two uroradiologists. These readers had 11 years and 1 year of experience in prostate imaging at the start of the database in 2008. Although patients were formally included in the database at the time of the prostatectomy, mp-MRI interpretation for purposes of the study was done on average 3 months later in order to avoid any recall from routine management of the patients. Additionally the readers were blinded to any clinical, biological and histopathological data concerning the patients, except the fact that they had undergone a prostatectomy.

First, readers noted all suspicious focal abnormalities (FAs) and localised them using a 27-regions-of-interest diagram, as recommended by a European consensus

panel [20]. In the peripheral zone (PZ), all FAs showing low-signal intensity on T2w images and/or ADC maps, and/or showing early enhancement on DCE images were taken into consideration. In the transition zone (TZ), only homogeneous low-signal intensity areas on T2w images, with ill-defined margins, no visible capsule and no cystic component [23–25] were interpreted as suspicious. ADC maps and raw DCE images were assessed only visually. Quantitative ADC values were not used to diagnose cancer. No enhancement parametric map was generated.

Second, the degree of suspicion of a given FA was assessed using a five-level subjective suspicion score (SSS: 0, definitely benign; 1, likely benign; 2, indeterminate; 3, likely malignant; 4, definitely malignant), as recommended by several European guidelines [18, 20]. No clear diagnostic criteria have yet been assigned to the five categories of the SSS. In the current study, areas with normal signal on all sequences were assigned a default SSS of 0/4 (definitely benign) and were not taken into account in the analysis. FAs that were, by definition, areas with abnormal signal at least on one sequence received an SSS of at least 1/4. Typically, nodules with typical malignant appearance on all three sequences received a 4/4 score (definitely malignant).
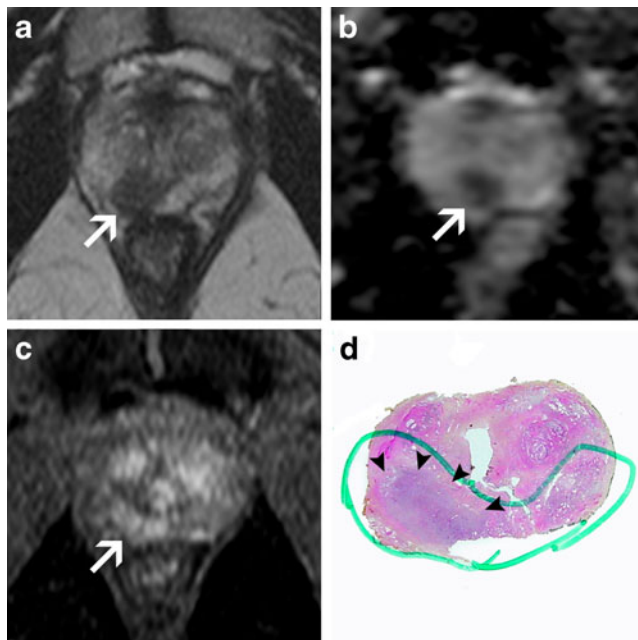
The distribution of the other combinations of signal abnormalities in the 1–3/4 categories was left to the readers' appreciation.

Finally, readers specified the presence and degree (none, minimal, marked) of post-biopsy blood artefact in near vicinity of each FA, as shown on the first (unenhanced) dynamic acquisition.

MR histological correlation

Histopathological and mp-MRI findings were then correlated by the readers and the uropathologist. First, the readers and the uropathologist reviewed the MR images together and the readers disclosed the FAs they had noted and their location. Then, the uropathologist decided which FAs matched histological cancers and which did not, using side-by-side comparison and taking into consideration as many landmarks (e.g. cysts, hyperplasia nodules, ejaculatory ducts) as possible. Matching FAs were considered true positives only if their largest diameter was within 50–150 % of the largest diameter of the corresponding histological cancer. Otherwise, the FA was considered an FP and the cancer a false negative (FN). In the case of FPs, the pathologist reviewed the whole-mount sections a second time to assess if a benign condition could explain the MR abnormality.
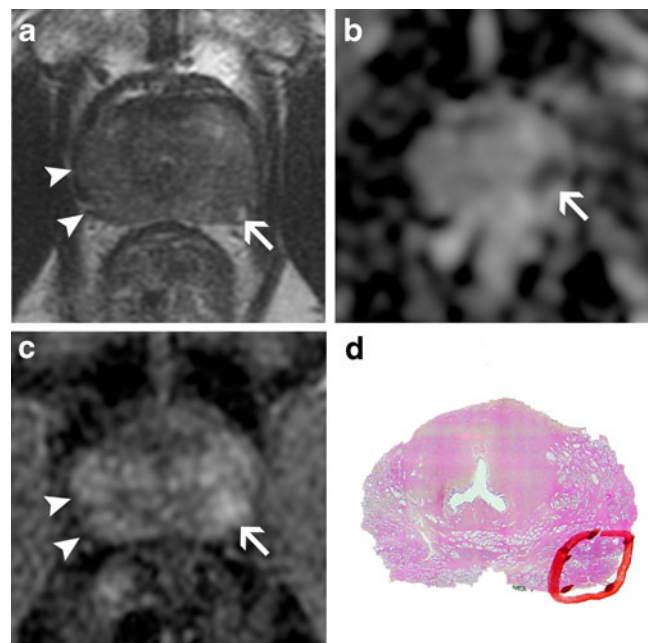

Fig. 1 Multiparametric axial MR images obtained on scanner A at 1.5 T (**a** T2w image; **b** ADC map; **c** DCE image) and histopathological whole-mount section (**d**) in a 62-year-old patient with a PSA level of 5.3 ng/ml. Both readers attributed a maximal SSS of 4 to the nodular focal abnormality in the right peripheral zone (**a–c**, *arrow*). Whole-mount section showed a Gleason 7 (3+4) cancer with a mixed architecture (**d**, *green outline*). Note that only the dense component (**d**, *arrowheads*) was visible at MRI, leading to a substantial underestimation of tumour volume

Fig. 2 Multiparametric axial MR images obtained on scanner B at 3 T (**a** T2w image; **b** ADC map; **c** DCE image) and histopathological whole-mount section (**d**) in a 53-year-old patient with a PSA level of 7 ng/ml. Readers 1 and 2 gave an SSS of 3 in the left peripheral zone (**a–c**, *arrow*). Reader 2 noted an additional abnormality in the right PZ with a SSS of 2 (**a–c**, *arrowheads*). Whole-mount section showed a Gleason 7 (3+4) cancer with a mixed architecture (**d**, *red outline*). In the right PZ, only high-grade prostate intraepithelial neoplasia was visible at pathology

Table 2 Tumour detection rates on mp-MRI as a function of imaging and histological parameters

			Tumour detection rate	
			Reader 1	Reader 2
Tumour location		Peripheral zone	187/296 (63 %)	168/296 (57 %)
		Transition zone	27/66 (41 %)	24/66 (36 %)
Tumour volume		<0.05 cc	13/46 (28 %)	6/46 (13 %)
		0.05–0.5 cc	53/141(38 %)	46/141 (33 %)
		0.5–2 cc	76/100 (76 %)	70/100 (70 %)
		>2 cc	72/75 (96 %)	70/75 (93 %)
Tumour Gleason score		5	7/21 (33 %)	5/21 (24 %)
		6	66/181 (36.5 %)	51/181 (28 %)
		7	96/113 (85 %)	91/113 (81 %)
		8–9	45/47 (96 %)	45/47 (96 %)
Tumour histological architecture		Dense	71/108 (66 %)	65/108 (60 %)
		Mixed	123/200 (61.5 %)	109/200 (54.5 %)
		Infiltrative	10/25 (40 %)	10/25 (40 %)
		Lobulated	10/29 (34.5 %)	8/29 (28 %)
Imaging field		1.5 T	99/157 (63 %)	86/157 (55 %)
		3 T	115/205 (56 %)	106/205 (52 %)
Coils used		Pelvic phased-array	150/240 (62.5 %)	131/240 (55 %)
		Pelvic phased-array and endorectal	64/122 (52.5 %)	61/122 (50 %)

Statistical analysis

Generalised linear mixed models (GLMM) were used to detect the influence regarding the FN and FP prediction of the following factors: tumour Gleason score, tumour histological volume, tumour architecture, tumour location (PZ vs TZ), field strength (1.5 T vs 3 T), coils used for imaging (PPA alone vs combined endorectal-PPA coils), patient age, preoperative PSA value and tumour pT stage. Individual random effects were used in order to take into account the intra-patient correlation. The model

Table 3 Influence of tumour location, volume, architecture and Gleason score on tumour detection at mp-MRI (multivariate analysis)

		Reader 1			Reader 2		
		OR	P value	95 % CI	OR	P value	95 % CI
Location	TZ [a]	1	–	–	1	–	–
	PZ	2.4	0.004	[1.28–4]	2.3	0.003	[1.25–3.97]
Histological volume	<0.05 cc [a]	1	–	–	1	–	–
	0.05–0.5 cc	1	0.8	[0.53–2.35]	3	0.01	[1.19–9.74]
	0.5–2 cc	5.4	10^{-6}	[2.48–12.08]	13.8	10^{-10}	[5.2–43.5]
	>2 cc	31.6	10^{-13}	[9.5–139.9]	88	10^{-16}	[24.3–407]
Architecture	Dense [a]	1	–	–	1	–	–
	Mixed	0.85	0.6	[0.5–1.43]	0.75	0.2	[1.19–9.74]
	Infiltrative	0.36	0.03	[0.13–0.97]	0.37	0.04	[5.2–43.5]
	Lobulated	0.38	0.03	[0.15–0.96]	0.25	0.002	[24.3–407]
Gleason score	5	1.05	0.99	[0.4–2.9]	0.81	0.8	[0.2–2.5]
	6 [a]	1	–	–	1	–	–
	7	8.7	10^{-6}	[4.7–16.5]	10.9	10^{-16}	[6.1–20.2]
	≥8	37.7	10^{-14}	[9.3–329]	59.2	10^{-16}	[14.6–519]

PZ peripheral zone, *TZ* transition zone, *OR* odds ratio

[a] Used as reference for the calculation of the odds ratio

Table 4 Tumour detection rate at multiparametric MRI as a function of the tumour Gleason score, the tumour histological volume and the imaging field

Field	Volume (cc)	Reader 1					Reader 2				
		Gleason score					Gleason score				
		5	6	7	8–9	Total	5	6	7	8–9	Total
1.5 T	<0.05	–	5/14 (36 %)	–	–	5/14 (36 %)	–	1/14 (7 %)	–	–	1/14 (7 %)
	0.05–0.5	1/3 (33 %)	15/46 (33 %)	7/13 (54 %)	1/1 (100 %)	24/63 (38 %)	1/3 (33 %)	10/46 (22 %)	6/13 (46 %)	1/1 (100 %)	18/63 (29 %)
	0.5–2	1/2 (50 %)	6/12 (50 %)	26/28 (93 %)	6/6 (100 %)	39/48 (81 %)	1/2 (50 %)	4/12 (33 %)	25/28 (89 %)	6/6 (100 %)	36/48 (75 %)
	>2	1/1 (100 %)	3/3 (100 %)	15/16 (94 %)	12/12 (100 %)	31/32 (97 %)	1/1 (100 %)	3/3 (100 %)	15/16 (94 %)	12/12 (100 %)	31/32 (97 %)
	Total	3/6 (50 %)	29/75 (39 %)	48/57 (84 %)	19/19 (100 %)	99/157 (63 %)	3/6 (50 %)	18/75 (24 %)	46/57 (81 %)	19/19 (100 %)	86/157 (55 %)
3 T	<0.05	2/6 (33 %)	6/25 (24 %)	–	0/1 (0 %)	8/32 (25 %)	1/6 (17 %)	4/25 (16 %)	–	0/1 (0 %)	5/32 (16 %)
	0.05–0.5	1/3 (33 %)	15/58 (26 %)	10/14 (71 %)	3/3 (100 %)	29/78 (37 %)	1/3 (33 %)	15/58 (26 %)	9/14 (64 %)	3/3 (100 %)	28/78 (36 %)
	0.5–2	0/4 (0 %)	12/17 (71 %)	19/23 (83 %)	7/8 (87.5 %)	37/52 (71 %)	0/4 (0 %)	10/17 (59 %)	17/23 (74 %)	7/8 (87.5 %)	34/52 (65 %)
	>2	1/2 (50 %)	4/6 (67 %)	19/19 (100 %)	16/16 (100 %)	41/43 (95 %)	0/2 (0 %)	4/6 (67 %)	19/19 (100 %)	16/16 (100 %)	39/43 (91 %)
	Total	4/15 (27 %)	37/106 (35 %)	48/56 (86 %)	26/28 (93 %)	115/205 (56 %)	2/15 (13 %)	33/106 (31 %)	45/56 (80 %)	26/28 (93 %)	106/205 (52 %)

Table 5 Tumour detection rate at multiparametric MRI as a function of the tumour Gleason score, the tumour histological volume and the type of coils used

Coil	Volume (cc)	Reader 1					Reader 2				
		Gleason score					Gleason score				
		5	6	7	8–9	Total	5	6	7	8–9	Total
PPA	<0.05	1/1 (100 %)	7/22 (32 %)	–	0/1 (0 %)	8/24 (33 %)	0/1 (0 %)	1/22 (4.5 %)	–	0/1 (0 %)	1/24 (4.2 %)
	0.05–0.5	1/4 (25 %)	18/65 (28 %)	13/22 (59 %)	1/1 (100 %)	33/92 (36 %)	2/4 (50 %)	14/65 (21.5 %)	11/22 (50 %)	1/1 (100 %)	28/92 (30 %)
	0.5–2	1/4 (25 %)	9/17 (53 %)	36/38 (95 %)	10/10 (100 %)	56/69 (81 %)	1/4 (25 %)	6/17 (35 %)	32/38 (84 %)	10/10 (100 %)	49/69 (71 %)
	>2	1/1 (100 %)	6/7 (86 %)	26/27 (96 %)	20/20 (100 %)	53/55 (96 %)	1/1 (100 %)	6/7 (86 %)	26/27 (96 %)	20/20 (100 %)	53/55 (96 %)
	Total	4/10 (40 %)	40/111 (36 %)	75/87 (86 %)	31/32 (97 %)	150/240 (62.5 %)	4/10 (40 %)	27/111 (24 %)	69/87 (79 %)	31/32 (97 %)	131/240 (55 %)
PPA + ER	<0.05	1/5 (20 %)	4/17 (23.5 %)	–	–	5/22 (23 %)	1/5 (20 %)	4/17 (23.5 %)	–	–	5/22 (23 %)
	0.05–0.5	1/2 (50 %)	12/39 (31 %)	4/5 (80 %)	3/3 (100 %)	20/49 (41 %)	0/2 (0 %)	11/39 (28 %)	4/5 (80 %)	3/3 (100 %)	18/49 (37 %)
	0.5–2	0/2 (0 %)	9/12 (75 %)	9/13 (69 %)	3/4 (75 %)	21/31 (68 %)	0/2 (0 %)	8/12 (67 %)	10/13 (77 %)	3/4 (75 %)	21/31 (68 %)
	>2	1/2 (50 %)	1/2 (50 %)	8/8 (100 %)	8/8 (100 %)	18/20 (90 %)	0/2 (0 %)	1/2 (50 %)	8/8 (100 %)	8/8 (100 %)	17/20 (85 %)
	Total	3/11 (27 %)	26/70 (37 %)	21/26 (81 %)	14/15 (93 %)	64/122 (52.5 %)	1/11 (9 %)	24/70 (34 %)	22/26 (85 %)	14/15 (93 %)	61/122 (50 %)

PPA Pelvic phased-array coil, *PPA + ER* combination of pelvic phased-array and endorectal coil

selection was performed using the likelihood ratio and the quasi-alike information criterion. Each regression coefficient was also tested using the Wald test. All GLMM models were calculated using the R package lme4. The odds ratios (ORs) were computed to quantify the predictive ability of factors. Agreement between readers' SSS score was measured with the kappa coefficient. $P<0.05$ was considered statistically significant and all confidence intervals (CI) were computed to 95 %.

Results

MR findings

Three hundred and sixty-nine FAs were described by reader 1, and 322 by reader 2. The proportion of FAs with a SSS of 1/4, 2/4, 3/4 and 4/4 were 22 % (81/369), 28 % (103/369), 25 % (93/369) and 25 % (92/369) for reader 1 and 9 % (30/322), 30 % (97/322), 31 % (100/322) and 30 % (95/322) for reader 2. The scoring concordance was moderate (kappa=0.4, $P=$ 0.02). Minimal and marked post-biopsy haemorrhage was visible in near vicinity of respectively 29 and 13 FAs for reader 1, and 31 and 30 FAs for reader 2.

Histological findings

The pathological T stage was pT0 in 3 (2 %) patients, pT2a in 13 (7 %), pT2b in 5 (3 %), pT2c in 78 (44.5 %), pT3a in 57 (32.5 %) and pT3b in 19 (11 %).

Pathological examination found 362 tumours (mean, 2.07 per patient). The Gleason score was 5 in 21 (6 %) tumours, 6 in 181 (50 %), 7 in 113 (31 %), 8 in 26 (7 %) and 9 in 21 (6 %). Sixty-six (18 %) tumours were in the TZ and 296 (82 %) in the PZ. The histological architecture was dense in 107 (30 %) tumours, mixed in 201 (55 %), infiltrative in 25 (7 %) and lobulated in 29 (8 %). Tumour volume was <0.05 cc (cm^3) in 46 (12.5 %) tumours, between 0.05 cc and 0.5 cc in 141 (39 %), between 0.5 cc and 2 cc in 100 (27.5 %) and >2 cc in 75 (21 %). The mean and median tumour volumes were 1.4 cc and 0.5 cc respectively (range, 0.04–15.7 cc).

MR histological correlation

Factors influencing tumour detection

Overall mp-MRI tumour detection rates were 59 % (214/362) and 53 % (192/362) for reader 1 and 2 respectively (Figs. 1 and 2).

Table 2 shows, for both readers, the tumour detection rates expressed separately as a function of the histological characteristics of the tumour, the imaging field and the coils used.

At multivariate analysis, detection rates were significantly influenced, for both readers, by tumour Gleason score, histological volume, histological architecture and location ($P<0.0001$ for all characteristics and readers; Table 3). Field strength, coils used, patient age, preoperative PSA value and pT stage did not significantly influence tumour detection.

Tables 4 and 5 show, for both readers, the breakdown of tumour detection rates as a function of tumour Gleason score and histological volume, at 1.5 T and 3 T (Table 4) and with and without an endorectal coil (Table 5). Overall detection rates for tumours of <0.5 cc, 0.5–2 cc and >2 cc were 33–45/155 (21–29 %), 15–19/35 (43–54 %) and 8–9/12 (67–75 %) for Gleason ≤6, 17/27 (63 %), 42–45/51 (82–88 %) and 34/35 (97 %) for Gleason 7 and 4/5 (80 %), 13/14 (93 %) and 28/28 (100 %) for Gleason ≥8 cancers respectively.

Factors influencing false positive findings

FP rates were 42 % (155/369) and 40 % (130/322) for reader 1 and 2 respectively.

Main causes of FP findings included active or chronic prostatitis, post-inflammatory glandular atrophy and high-grade prostate intra-epithelial neoplasia (Table 6). There was at least one retrospective explanation for 111/155 (72 %) and 103/130 (79 %) FPs for reader 1 and 2 respectively. At multivariate analysis, the field strength and coils used did not significantly influence the FP rate for reader 1. For reader 2, the use of combined PPA-

Table 6 Causes of multiparametric MRI false positive findings

	Reader 1	Reader 2
Active or chronic prostatitis	41/111 (37 %)	38/103 (37 %)
Post-inflammatory glandular atrophy	33/111 (29 %)	19/103 (18.5 %)
High-grade prostate intra-epithelial neoplasia	29/111 (26 %)	27/103 (26 %)
Adenomatous lesions	12/111 (11 %)	24/103 (23 %)
Fibrosis or fibro-muscular stroma	9/111 (8 %)	6/103 (6 %)
Myomatous lesions	7/111 (6 %)	8/103 (8 %)
Adenosis nodules	7/111 (6 %)	11/103 (11 %)
No histological abnormality but bleeding artefact at MRI	4/111 (4 %)	10/103 (10 %)

Table 7 Percentage of malignant FAs as a function of the subjective suspicion score (*SSS*)

	SSS1	SSS2	SSS3	SSS4
Reader 1	21/81 (26 %)	42/103 (41 %)	61/93 (66 %)	90/92 (98 %)
Reader 2	2/30 (7 %)	26/97 (27 %)	72/100 (72 %)	92/95 (97 %)

endorectal coils was significantly associated ($P<0.003$) with a lower rate of FPs.

Value of the SSS

The SSS was a significant predictor of the malignant nature of FAs for both readers ($P<0.005$, Table 7). Compared with FAs with an SSS of 1/4, FAs with an SSS of 2/4, 3/4 and 4/4 had ORs for being malignant of 1.96 (95% CI, 1–3.9), 5.5 (2.7–11) and 123 (28.9–1,145) for reader 1 and 4.7 (1–43.5), 34 (7.9–322) and 506 (71–7,986) for reader 2.

The SSS was also a significant predictor of tumour aggressiveness among cancers detected ($P<0.00001$, Table 8). Compared with malignant FAs with an SSS of 1–2/4, malignant FAs with a SSS of 3/4 and 4/4 had ORs of having a Gleason score ≥7 of 3.74 (95% CI, 1.6–7) and 24.3 (8–52) for reader 1 and 1.5 (0.6–3.3) and 7.8 (2.6–20.6) for reader 2.

Discussion

The purpose of our study was to evaluate the influence of imaging parameters and tumours' histological characteristics on mp-MRI prostate cancer detection. We found four significant predictors of tumour detection: the tumour location, histological architecture, Gleason score and histological volume.

The fact that TZ tumours were significantly less detected comes as no surprise, as they are reputed to be difficult to distinguish from benign hyperplasia nodules, even if specific T2w image features have been recently described [23–25].

The influence of the Gleason score on prostate cancer detection on mp-MRI has already been assessed in many studies. MR parameters such as tumour-muscle signal intensity ratio on T2w imaging [26], ADC value [27–32] or (choline + creatine)/citrate ratio on MRS [33, 34] have been found to be correlated with tumour Gleason score and/or aggressive behaviour. Girouin et al. [8] reported detection rates for Gleason 6, 7 and ≥8 cancers of 11.8–16.9 %, 57.4–67.2 % and 64.1–73.1 % respectively on T2w imaging and 29.7–33.9 %, 77.5–80.7 % and 96.1–96.7 % on DCE

imaging. Two recent studies also found that mp-MRI including T2w, Dw and DCE imaging, with [10] or without [11] MRS had a significantly better sensitivity for cancers with higher Gleason scores. Our results (Tables 4 and 5) strongly suggest that mp-MRI is particularly sensitive for cancers containing grades 4–5 carcinoma. In this respect, it could have been interesting to assess detection rates of Gleason 3+4 and 4+3 tumours that seem to exhibit significantly different prognosis [35, 36]. This analysis was not possible because of the small number of cases involved, but as our database grows in time, it will become possible.

The impact of tumour volume on tumour detection on mp-MRI has seldom been evaluated [13], maybe because the calculation of the histological tumour volume is difficult [37]. If tumour surface on each whole-mount section can be easily measured, thickness of histological blocks, and thus spacing between whole-mounts, is usually not precisely monitored. We paid particular attention to this point by monitoring the distance between whole-mount sections in order to estimate tumour volume as accurately as possible. We did not use any correction factor for tissue shrinkage because these correction factors remain controversial and fall within the wide range of 1.14–1.5 in the existing literature [38, 39]. Tissue shrinkage probably varies from one laboratory to another, possibly from one prostate to another. Only an estimation of the shrinkage on a patient-by-patient basis could provide precise evaluation of tumour volume. We are currently trying to develop a precise method for MR-pathological co-registration that remains compatible with routine workflow and therefore allows estimation of tissue shrinkage for each individual patient [40]. In the meantime, our results may slightly overestimate mp-MRI performance because tissue shrinkage is not taken into account.

Tumour architecture is a known predictor of detection at mp-MRI [11, 14], with dense tumours better detected, probably because T2w and Dw imaging are particularly sensitive to increased cellularity [15]. It remains unclear, however, whether tumour architecture is associated with tumour aggressiveness or not.

The influence of the imaging field strength and coils on tumour detection remains unclear. The use of high-field

Table 8 Percentage of Gleason ≥7 tumours in malignant FAs as a function of the subjective suspicion score (*SSS*)

	SSS1	SSS2	SSS3	SSS4
Reader 1	7/21 (33 %)	14/42 (33 %)	39/61 (64 %)	81/90 (90 %)
Reader 2	2/2 (100 %)	12/26 (46 %)	42/72 (59 %)	80/92 (87 %)

strength and/or the use of the endorectal coil provide an excellent signal-to-noise ratio and are associated with improved image quality or depiction of prostate anatomy [17, 41, 42]. Local staging seems improved by the use of the endorectal coil at 1.5 T and at 3 T [17, 41]. The comparison of the staging accuracy at 1.5 T with an endorectal coil and at 3 T with PPA coils showed similar results [43, 44]. As a result, the use of the endorectal coil remains the state of the art at 1.5 T, whereas it is usually considered optional at 3 T [18]. Nevertheless, data on the influence of the use of high-field strength or the endorectal coil on tumour depiction are scarce and limited to T2w imaging [17, 44, 45]. To our knowledge, no randomised study or any direct comparison in the same patients have ever assessed the tumour detection obtained with mp-MRI (i.e. including not only T2w but also Dw, DCE imaging and/or MRS) at 1.5 T versus 3 T or with versus without an endorectal coil. In this study, we aggregated data from three different MR systems using different field strength and coil configuration. Although this induces heterogeneity in the series, it also more closely reflects current routine practice and allows the assessment of the impact of technical imaging factors on tumour detection through data stratification. Our results strongly suggest that field strength and coil configuration have little influence on tumour detection compared with other factors such as histological characteristics. This is in line with the excellent results in tumour detection published at 1.5 T with PPA alone [3, 46]. We believe that this is due to the fact that tumours that are not detected at current mp-MRI are overlooked not because of a lack of signal but rather because of a lack of contrast with neighbouring normal tissue.

We characterised all visible FAs using a suspicion score based on a five-level scale, as recommended by several European guidelines [18, 20]. This score was a highly significant predictor of malignancy for both readers, and could be a way of addressing the issue of the lack of specificity of mp-MRI. Indeed, respectively 78 % and 76 % of FPs of readers 1 and 2 had a SSS of 1–2/4 (Table 7). We displayed our results by taking into account all FAs, whatever their SSS. Had we chosen a threshold of 1/4 or 2/4 for diagnosis of malignancy, the PF rate would have been largely improved, but at the expense of a slight decrease in the tumour detection rate (Table 7). However, we do not think that routine mp-MRI results should be binary (benign/malignant), but rather than the SSS assigned to every visible FA should be disclosed to the corresponding urologist in order to guide more precisely patient management. Indeed, we found the SSS to be not only a significant predictor of malignancy but also of tumour aggressiveness (Table 8). In other words, a FA that has a typical appearance of cancer on all sequences (SSS of 4/4) has not only a high probability of being malignant but also of being a Gleason ≥7 tumour. This finding might have important consequences on the management of candidates to repeat biopsy, active surveillance, or focal therapy.

Nevertheless, the SSS remains subjective and the good results obtained in a department of uroradiology might not be reproduced in non-specialised institutions. Therefore, suspicion scores based on more objective criteria are needed [47]. The recently published PiRads scoring system [18] might be less subjective, but this remains to be assessed.

Our study has some limitations. Firstly, we included only patients who underwent prostatectomy, which inevitably induced a selection bias. However, this bias was limited by the fact that we took into account all cancer foci in the specimens and not only the index tumour, which was usually the easiest to detect. Secondly, MR-histopathological correlation remains difficult because of the difference in angle section between whole-mounts and MR images. Despite all the care taken to ensure a match between histological cancer foci and MR FAs, mismatches might have occurred. Thirdly, we did not use MRS. Although this technique has yielded interesting results [4, 34, 48], its additional value to mp-MRI remains questionable [49, 50]. Furthermore, its long acquisition time makes it difficult to use in daily practice. As a result, MRS is not routinely performed at our institution.

In conclusion, prostate cancer location, histological volume, Gleason score and histological architecture were independent significant predictors of tumour detection on mp-MRI, whereas the use of a high field strength and/or endorectal coil was not. The use of a five-grade subjective score can significantly stratify the risk of malignancy and aggressiveness of an abnormality seen on mp-MRI. We believe that these findings will be useful in determining the role of mp-MRI before prostate biopsy or in the management of candidates for active surveillance or focal therapy.

References

1. Lindner U, Trachtenberg J, Lawrentschuk N (2010) Focal therapy in prostate cancer: modalities, findings and future considerations. Nat Rev Urol 7:562–571
2. Rouviere O, Gelet A, Crouzet S, Chapelon JY (2012) Prostate focused ultrasound focal therapy—imaging for the future. Nat Rev Clin Oncol 9:721-727
3. Kirkham AP, Emberton M, Allen C (2006) How good is MRI at detecting and characterising cancer within the prostate? Eur Urol 50:1163–1174, discussion 1175
4. Turkbey B, Pinto PA, Mani H et al (2010) Prostate cancer: value of multiparametric MR imaging at 3T for detection—histopathologic correlation. Radiology 255:89–99
5. Sciarra A, Barentsz J, Bjartell A et al (2011) Advances in magnetic resonance imaging: how they are changing the management of prostate cancer. Eur Urol 59:962–977
6. Riches SF, Payne GS, Morgan VA et al (2009) MRI in the detection of prostate cancer: combined apparent diffusion coefficient, metabolite ratio, and vascular parameters. AJR Am J Roentgenol 193:1583–1591

7. Heidenreich A (2011) Consensus criteria for the use of magnetic resonance imaging in the diagnosis and staging of prostate cancer: not ready for routine use. Eur Urol 59:495–497

8. Girouin N, Mege-Lechevallier F, Tonina Senes A et al (2007) Prostate dynamic contrast-enhanced MRI with simple visual diagnostic criteria: is it reasonable? Eur Radiol 17:1498–1509

9. Cheikh AB, Girouin N, Colombel M et al (2009) Evaluation of T2-weighted and dynamic contrast-enhanced MRI in localizing prostate cancer before repeat biopsy. Eur Radiol 19:770–778

10. Turkbey B, Mani H, Shah V et al (2011) Multiparametric 3T prostate magnetic resonance imaging to detect cancer: histopathological correlation using prostatectomy specimens processed in customized magnetic resonance imaging based molds. J Urol 186:1818–1824

11. Rosenkrantz AB, Mendrinos S, Babb JS, Taneja SS (2012) Prostate cancer foci detected on multiparametric magnetic resonance imaging are histologically distinct from those not detected. J Urol 187:2032-2038

12. Isebaert S, Van den Bergh L, Haustermans K et al (2012) Multiparametric MRI for prostate cancer localization in correlation to whole-mount histopathology. J Magn Reson Imaging. doi:10.1002/jmri.23938

13. Villers A, Puech P, Mouton D, Leroy X, Ballereau C, Lemaitre L (2006) Dynamic contrast enhanced, pelvic phased array magnetic resonance imaging of localized prostate cancer for predicting tumor volume: correlation with radical prostatectomy findings. J Urol 176:2432–2437

14. Langer DL, van der Kwast TH, Evans AJ et al (2008) Intermixed normal tissue within prostate cancer: effect on MR imaging measurements of apparent diffusion coefficient and T2–sparse versus dense cancers. Radiology 249:900–908

15. Tan CH, Wang J, Kundra V (2011) Diffusion weighted imaging in prostate cancer. Eur Radiol 21:593–603

16. Kayhan A, Fan X, Oommen J, Oto A (2010) Multi-parametric MR imaging of transition zone prostate cancer: imaging features, detection and staging. World J Radiol 2:180–187

17. Heijmink SW, Futterer JJ, Hambrock T et al (2007) Prostate cancer: body-array versus endorectal coil MR imaging at 3T—comparison of image quality, localization, and staging performance. Radiology 244:184–195

18. Barentsz JO, Richenberg J, Clements R et al (2012) ESUR prostate MR guidelines 2012. Eur Radiol 22:746–757

19. Kim CK, Park BK, Kim B (2010) Diffusion-weighted MRI at 3T for the evaluation of prostate cancer. AJR Am J Roentgenol 194:1461–1469

20. Dickinson L, Ahmed HU, Allen C et al (2011) Magnetic resonance imaging for the detection, localisation, and characterisation of prostate cancer: recommendations from a European consensus meeting. Eur Urol 59:477–494

21. Rouviere O, Hartman RP, Lyonnet D (2006) Prostate MR imaging at high-field strength: evolution or revolution? Eur Radiol 16:276–284

22. Shukla-Dave A, Hricak H, Eberhardt SC et al (2004) Chronic prostatitis: MR imaging and 1H MR spectroscopic imaging findings—initial observations. Radiology 231:717–724

23. Akin O, Sala E, Moskowitz CS et al (2006) Transition zone prostate cancers: features, detection, localization, and staging at endorectal MR imaging. Radiology 239:784–792

24. Lemaitre L, Puech P, Poncelet E et al (2009) Dynamic contrast-enhanced MRI of anterior prostate cancer: morphometric assessment and correlation with radical prostatectomy findings. Eur Radiol 19:470–480

25. Oto A, Kayhan A, Jiang Y et al (2010) Prostate cancer: differentiation of central gland cancer from benign prostatic hyperplasia by using diffusion-weighted and dynamic contrast-enhanced MR imaging. Radiology 257:715–723

26. Wang L, Mazaheri Y, Zhang J, Ishill NM, Kuroiwa K, Hricak H (2008) Assessment of biologic aggressiveness of prostate cancer: correlation of MR signal intensity with Gleason grade after radical prostatectomy. Radiology 246:168–176

27. Hambrock T, Somford DM, Huisman HJ et al (2011) Relationship between apparent diffusion coefficients at 3.0-T MR imaging and Gleason grade in peripheral zone prostate cancer. Radiology 259:453–461

28. Giles SL, Morgan VA, Riches SF, Thomas K, Parker C, deSouza NM (2011) Apparent diffusion coefficient as a predictive biomarker of prostate cancer progression: value of fast and slow diffusion components. AJR Am J Roentgenol 196:586–591

29. Woodfield CA, Tung GA, Grand DJ, Pezzullo JA, Machan JT, Renzulli JF 2nd (2010) Diffusion-weighted MRI of peripheral zone prostate cancer: comparison of tumor apparent diffusion coefficient with Gleason score and percentage of tumor on core biopsy. AJR Am J Roentgenol 194:W316–W322

30. Verma S, Rajesh A, Morales H et al (2011) Assessment of aggressiveness of prostate cancer: correlation of apparent diffusion coefficient with histologic grade after radical prostatectomy. AJR Am J Roentgenol 196:374–381

31. Oto A, Yang C, Kayhan A et al (2011) Diffusion-weighted and dynamic contrast-enhanced MRI of prostate cancer: correlation of quantitative MR parameters with Gleason score and tumor angiogenesis. AJR Am J Roentgenol 197:1382–1390

32. Turkbey B, Shah VP, Pang Y et al (2011) Is apparent diffusion coefficient associated with clinical risk scores for prostate cancers that are visible on 3-T MR images? Radiology 258:488–495

33. Zakian KL, Sircar K, Hricak H et al (2005) Correlation of proton MR spectroscopic imaging with gleason score based on step-section pathologic analysis after radical prostatectomy. Radiology 234:804–814

34. Crehange G, Parfait S, Liegard M et al (2011) Tumor volume and metabolism of prostate cancer determined by proton magnetic resonance spectroscopic imaging at 3T without endorectal coil reveal potential clinical implications in the context of radiation oncology. Int J Radiat Oncol Biol Phys 80:1087–1094

35. Chan TY, Partin AW, Walsh PC, Epstein JI (2000) Prognostic significance of Gleason score 3+4 versus Gleason score 4+3 tumor at radical prostatectomy. Urology 56:823–827

36. Tollefson MK, Leibovich BC, Slezak JM, Zincke H, Blute ML (2006) Long-term prognostic significance of primary Gleason pattern in patients with Gleason score 7 prostate cancer: impact on prostate cancer specific survival. J Urol 175:547–551

37. Noguchi M, Stamey TA, McNeal JE, Yemoto CE (2000) Assessment of morphometric measurements of prostate carcinoma volume. Cancer 89:1056–1064

38. Schned AR, Wheeler KJ, Hodorowski CA et al (1996) Tissue-shrinkage correction factor in the calculation of prostate cancer volume. Am J Surg Pathol 20:1501–1506

39. Stamey TA, McNeal JE, Freiha FS, Redwine E (1988) Morphometric and clinical studies on 68 consecutive radical prostatectomies. J Urol 139:1235–1241

40. Hughes C, Rouviere O, Mege-Lechevallier F, Souchon R, Prost R (2012) Robust alignment of prostate histology slices with quantified accuracy. IEEE Trans Biomed Eng 60:281-291

41. Futterer JJ, Engelbrecht MR, Jager GJ et al (2007) Prostate cancer: comparison of local staging accuracy of pelvic phased-array coil alone versus integrated endorectal-pelvic phased-array coils. Local staging accuracy of prostate cancer using endorectal coil MR imaging. Eur Radiol 17:1055–1065

42. Bloch BN, Rofsky NM, Baroni RH, Marquis RP, Pedrosa I, Lenkinski RE (2004) 3 Tesla magnetic resonance imaging of the prostate with combined pelvic phased-array and endorectal coils; Initial experience(1). Acad Radiol 11:863–867

43. Torricelli P, Cinquantini F, Ligabue G, Bianchi G, Sighinolfi P, Romagnoli R (2006) Comparative evaluation between external phased array coil at 3T and endorectal coil at 1.5T: preliminary results. J Comput Assist Tomogr 30:355–361

44. Beyersdorff D, Taymoorian K, Knosel T et al (2005) MRI of prostate cancer at 1.5 and 3.0T: comparison of image quality in tumor detection and staging. AJR Am J Roentgenol 185:1214–1220

45. Hricak H, White S, Vigneron D et al (1994) Carcinoma of the prostate gland: MR imaging with pelvic phased-array coils versus integrated endorectal—pelvic phased-array coils. Radiology 193:703–709

46. Ahmed HU, Kirkham A, Arya M et al (2009) Is it time to consider a role for MRI before prostate biopsy? Nat Rev 6:197–206

47. Rouviere O, Papillard M, Girouin N et al (2012) Is it possible to model the risk of malignancy of focal abnormalities found at prostate multiparametric MRI? Eur Radiol 22:1149–1157

48. Scheidler J, Hricak H, Vigneron DB et al (1999) Prostate cancer: localization with three-dimensional proton MR spectroscopic imaging—clinicopathologic study. Radiology 213:473–480

49. Mazaheri Y, Shukla-Dave A, Hricak H et al (2008) Prostate cancer: identification with combined diffusion-weighted MR imaging and 3D 1H MR spectroscopic imaging—correlation with pathologic findings. Radiology 246:480–488

50. Weinreb JC, Blume JD, Coakley FV et al (2009) Prostate cancer: sextant localization at MR imaging and MR spectroscopic imaging before prostatectomy–results of ACRIN prospective multi-institutional clinicopathologic study. Radiology 251:122–133